Available online at www.sciencedirect.com
SCIENCE DIRECT®
Journal of Sound and Vibration 291 (2006) 1170–1185
JOURNAL OF SOUND AND VIBRATION
www.elsevier.com/locate/jsvi

Characterization of an experimental wavenumber fitting method for loss factor estimation using a viscoelastically damped structure ☆

Vikrant Palan[a], W. Steve Shepard Jr.[a,*], J. Gregory McDaniel[b]

[a]*The University of Alabama, Department of Mechanical Engineering, 290 Hardaway Hall, Box 870276, Tuscaloosa, AL 35487, USA*
[b]*Boston University, Department of Aerospace and Mechanical Engineering, 110 Cummington Street, Boston, MA 02215, USA*

Received 19 October 2004; received in revised form 1 July 2005; accepted 13 July 2005
Available online 8 September 2005

Abstract

This study presents the experimental characterization of a relatively new method used to measure the damping performance of a structure. The method evaluated is the complex wavenumber fitting method in which an analytical description of the response over the structure surface is adjusted to match experimental measurements of the response over the same region. In computing the analytical response, a large number of points on the structure can be considered without much expense. In measuring that response, though, one must consider both experimental complexity and measurement time when considering the number of sensor locations. The goal of the present study is to examine the number of measurement points needed in the complex wavenumber fitting method to obtain a loss factor of sufficient accuracy. To that end, the loss factor for a viscoelastically damped sandwich beam with intermediate bolts is determined for different numbers of measurement points. To facilitate this study, a scanning laser vibrometer is used to measure the response at many points on the structure. Then, the wavenumber is estimated by iteratively fitting an analytical wave description to the response. For various selected sets of response points, it is shown that this approach is sensitive to both the number of measurement points as well as the coherence of that data.

☆A portion of this work was presented at *2005 SAE Noise & Vibration Conference and Exhibition*, May 16–19, Traverse City, MI, USA.

*Corresponding author. Tel.: +1 205 348 0048; fax: +1 205 348 0483.
E-mail address: sshepard@eng.ua.edu (W.S. Shepard Jr.).

0022-460X/$ - see front matter
doi:10.1016/j.jsv.2005.07.028

Experimental examples are presented to demonstrate those effects. Recommendations for better signal-to-noise ratio using the scanning laser system are also provided.

1. Introduction

Resonant vibrations can be an important problem in structural design. When excited, these vibrations can lead to large vibration amplitudes that in turn produce excessive noise and vibrations in any attached equipment. Furthermore, these high vibration amplitudes often reduce the useful life of a structure due to fatigue. Consequently, there has been much interest in developing damping methods for reducing vibration. There has also been equal interest in the development of methods for experimentally characterizing the performance of those damping applications.

One experimental method recently developed for determining damping performance involves the iterative refinement of a structural wavenumber such that a wave model can be fitted to match measured test data [1]. Unlike the half-power method [2], this approach uses multiple measurements along the length of the wave field or the structure under consideration. With the half-power method and other conventional approaches, one is usually only able to measure the damping performance at a few discrete frequencies. With the iterative wavenumber approach, one can determine the damping performance over a range of frequencies. Previous research has discussed the positioning of the measurement locations for the wavenumber approach [1]. However, the minimum number of positions needed to obtain accurate results with the iterative method has not been addressed in detail. Furthermore, the impact of measurement coherence on the usefulness of the wavenumber technique has not been studied. Therefore, the objective of the work presented here is to examine the impact of the number of measurement locations and data coherence on the damping performance assessment provided by the iterative refinement technique. By determining the minimum number of positions required, the speed of experimental data collection can potentially be increased. Furthermore, the computational time required for this method can potentially be reduced when fewer measurements are required. More importantly, the accuracy of the method in measuring loss factor may be improved when a better understanding of the data requirements is obtained. The test specimen used to evaluate this method, which will be described below, is one that is particularly suited to this study.

A variety of damping techniques for the dissipation of unwanted acoustical and vibrational energy have been developed. The approach considered in this work is constrained layer damping (CLD). CLD provides for the dissipation of vibrational energy by the physical distortion of a layer of soft viscoelastic material sandwiched between the vibrating structure and a strong constraining layer. As the entire structure vibrates in flexure, the viscous damping layer is subjected to a shear deformation between the primary (base) structure and the constraining layer, as illustrated in Fig. 1. Due to the fact that the viscoelastic material exhibits hysteresis, the shear in the damping layer creates internal viscous friction that dissipates vibratory energy during each cycle of oscillation.

The experimental specimen used for this study is a viscoelastically damped sandwich beam with intermediate fasteners. An example of a conventional sandwich configuration consisting of two structural square tubes is illustrated in Fig. 2(a). Note that for this structure the damping layer is placed at the neutral axis to achieve large shear deformation. This shear deformation has the potential to provide improved system damping performance. When replacing a conventional structural member having almost no damping by a viscoelastic shear-damped beam, such as the one illustrated in the figure, a reduction in static stiffness may be expected. To address this stiffness issue and provide for improved construction methods, intermediate stiffeners, such as bolts or rivets, may be used as shown in Fig. 2(b). These fasteners may be placed at various positions along the length of the beam. With the insertion of these stiffeners, the viscoelastic layer will still provide damping, while the bolts in the system will impart the desired static rigidity.

The earliest relevant theoretical investigation of constrained layer damping was the work of Kerwin [3]. They defined the loss factor as the "normalized imaginary part of complex bending stiffness of the damping plate." Their work was basically restricted to the simply supported boundary condition. Later Kerwin and McQuillan [4] accounted for other boundary conditions by patching a correction factor to the results previously obtained. They concluded that the loss factor is inversely proportional to frequency and temperature, and is directly proportional to the thickness of the constraining layer. Studies related to the impact of stiffeners on damping performance can be found in Refs. [5,6]. Note that these studies considered only the effect of end stiffeners and required detailed information regarding the boundary conditions. Furthermore, these studies estimated loss factor at only the resonant frequencies. As mentioned earlier, the experimental method being analyzed in the present study overcomes some of these limitations.

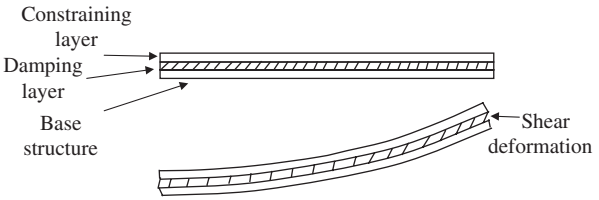

Fig. 1. Constrained layer damping treatment.

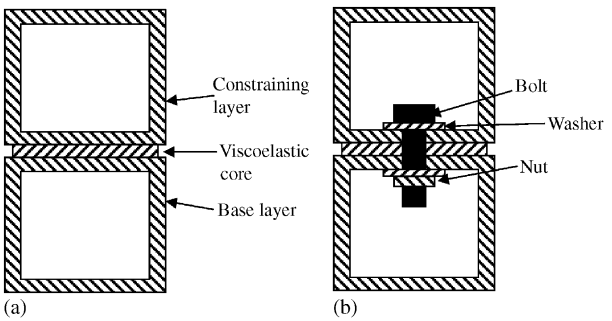

Fig. 2. Cross-section of the sandwich beam (a) with intermediate stiffeners (b).

In the following section, the experimental iterative wavenumber fitting method is briefly reviewed. Then, a description of the test specimen and test set-up is provided. Some important assumptions are also noted with regard to the application of the experimental method to the selected structure. Then, the loss factor estimation results for various data subsets will be examined in order to make an assessment of some of the requirements for the complex wavenumber measurement technique.

2. Iterative wavenumber fitting method

The measurement of loss factor based on the attenuation of vibrations with distance along the length of the structure is explained in the text by Cremer and Heckl [7]. Implementation of this method assumes that one can measure the decay in amplitude along the length of the structure through the measurement of that structure's response. Reflections from the ends of a finite length structure are not specifically addressed in that work. To address these issues, a wavenumber fitting algorithm was more formalized by McDaniel and Shepard [1]. The latter method requires no prior knowledge regarding the boundary conditions of the structure. Since that iterative wavenumber fitting algorithm is the subject of the present research, a brief overview of the technique is presented in this section.

The method, as described by McDaniel and Shepard, is based on determining the value of the complex wavenumber k for the wave propagating within the structure. Once this wavenumber is found, using the methods described below, the loss factor at the particular frequency of interest can be determined using the relationship

$$\eta = \frac{\mathrm{Im}\{k^4\}}{\mathrm{Re}\{k^4\}}. \tag{1}$$

To determine the wavenumber, this method requires measuring the vibratory response, D_m, at a number of positions m, along the length of the structure. The wavenumber is determined at each frequency by an iterative algorithm. The method essentially finds a complex wavenumber such that an analytical description of the response at each point, W_m, most closely approximates the measured response D_m at that same point. Once a purely real valued initial guess is determined for the wavenumber, the method adjusts the value of both the real and imaginary parts of the wavenumber until the computed wave field most closely matches the measured response. An iterative procedure is used to find the complex k. The resulting wavenumber is then used in Eq. (1) to determine the real-valued loss factor. The relationships used to find the complex wavenumber for a beam in flexure, which is the structure of interest, are now reviewed.

The flexural wave field W_m in a beam can be analytically described by

$$W_m = \sum_{n=1}^{N} \{F_n e^{ik_n x_m} + B_n e^{ik_n (L - x_m)}\} \quad \text{for } m = 1, 2, \ldots, M, \tag{2}$$

where x_m is the location of measurement m, and M is the total number of measurements. The subscript n represents the number of wave types that are assumed to propagate along the length of the beam. Since a fourth-order differential equation will be assumed to represent the sandwich

beam, both flexural and evanescent waves will be considered with $N = 2$. The wavenumbers of these two wave types may be related by a factor of i, that is, $k_e \approx ik_f$ where k_e and k_f are the wavenumbers for the evanescent and flexural waves, respectively. The coefficients F_n and B_n are the amplitudes of the forward and backward traveling waves, respectively. The effect of the boundary conditions is included in the coefficients F_n and B_n, while k_n represents the complex wavenumber. Note that either k_e or k_i may be used in Eq. (1). As a result, the complex wavenumber can simply be denoted by k_n. If the response is measured experimentally, there are five unknowns in Eq. (2): two forward traveling wave amplitudes $F_n(n = 1, 2)$, two backward traveling wave amplitudes $B_n(n = 1, 2)$, and the wavenumber. In the curve fitting algorithm, the complex wavenumber k_n is first guessed for a particular frequency, as described later, and the F_n and B_n are calculated by linear inversion of the equation

$$[[\phi][\beta]]\begin{Bmatrix}\{F_n\}\\ \{B_n\}\end{Bmatrix} = \{D\}, \tag{3}$$

where the terms of the propagation matrices $[\phi]$ and $[\beta]$ are given by

$$\phi_{mn} = \mathrm{e}^{ik_n x_m} \quad \text{and} \quad \beta_{mn} = \mathrm{e}^{ik_n(L-x_m)}, \tag{4}$$

and D_m is the measured response at the discrete locations along the length of the beam. Of course, x_n must match the lengthwise position of each of the measurement points. Once k_n, F_n, and B_n are estimated at the particular frequency of interest, the wave field W_m is reconstructed using Eq. (2) at various points along the beam. That is, the response can also be computed at locations other than the measurement location x_n. Since the analytical description W_m at each point is not expected to match the corresponding experimental measurement D_m exactly, a normalized mean square (NMSE) error ε is used to compare the accuracy of the model in describing the actual measured response

$$\varepsilon = \sqrt{\left(\sum_{m=1}^{M} |W_m - D_m|^2\right) / \left(\sum_{m=1}^{M} |D_m|^2\right)}. \tag{5}$$

This normalized error will be different depending on the real and imaginary component of the complex wavenumber. As a result, the above curve fitting process can be iteratively repeated by adjusting the real and imaginary parts of the complex wavenumber such that the error ε is minimized. A minimized ε implies a good estimation of k_n, F_n, and B_n for describing the measured response. The k_n corresponding to the minimum ε is then used in Eq. (1) to calculate the loss factor for that particular frequency.

In order to initiate the iteration process, one must have a rough estimate for the complex wavenumber at the first frequency of interest. The approach used here is to plot the logarithm of the normalized mean square error (NMSE) versus the real and imaginary parts of the complex wavenumber. This plot is of an error surface for a certain range of discrete values of the complex wavenumber. The combination of the real and the imaginary parts corresponding to the minimum NMSE is the most accurate starting guess for the wavenumber. Once the starting guess for the wavenumber is known, the iterative process to find the best fit for the vibrational response can be initiated. This computation method is now discussed.

Although there are a number of approaches that could be used to find the complex wavenumber over a range of frequencies, the approach used here starts at the highest frequency, where the technique is most likely to find an accurate value for the wavenumber. In the first pass of the technique, therefore, the wavenumber and loss factor at the highest frequency are determined. The minimization procedure is automated by using the MATLAB® function "fminsearch" to simultaneously adjust the real and imaginary parts of each k_n to minimize ε. The final complex valued k_n at that frequency is then used as the initial guess at the next lower frequency. The process then continues down to the lowest frequency using the most recently obtained k_n as the guess at the next lower frequency.

With a review of the iterative wavenumber fitting method complete, it is now beneficial to describe the test specimen used to evaluate this experimental method. A brief review of the basic equations used to estimate the loss factor during the design of the structure is also provided. The loss factor predictions found using these existing analytical formulations provide a basis for evaluating the results of the present study, which are described after the laboratory set-up is described.

3. Specimen description

For the test specimen, a 4.5 foot (1.4 m) long beam is selected where the base layer and the constraining layer is of the same dimensions. Both the base and constraining layers are 2″ (5 cm) hollow square tubes with 1/8″ (3.2 mm) thick walls. In order to fasten the two exterior layers through the viscoelastic layer, seven bolt holes and seven access holes have been drilled through the walls of each beam. A schematic denoting the location of these holes along the length of the beam is shown in Fig. 3(a). One wall of each beam contains 3/16″ (4.8 mm) diameter holes at each of the seven fastener location. This wall is the one that mates with the intermediate viscoelastic layer. The opposite wall of the beam has seven equally located 3/4″ (19 mm) diameter holes that are used for tooling access. Accessibility of the bolts and mating nuts via the 3/4″ holes is important during beam assembly and bolt torquing. The damping material used in the experiments is the elastomer ISODAMP™ C-1002 from EAR Specialty Composites [8]. Of course, this material has 3/16″ diameter holes at the same locations as the mating holes on the beam.

The dimensions of the beam were chosen using simple analytical calculations based on the relationships developed by Ungar [9]. While this formulation applies to an infinite length, simply supported beam with no intermediate stiffeners, the relative ease of its implementation provides a starting point for estimating loss factor for a beam that is freely suspended. As a result, the basic analysis tool is useful in choosing the beam and layer sizes such that the system loss factor can be expected to be a relatively high value in the frequency range of interest. A brief overview of these relations is provided below so that one can see how this formulation relates to the measurement of the loss factor described above.

For an infinitely long or simply supported constrained layer beam without stiffeners, subject to flexural sinusoidal motion, the system loss factor is given by [9]

$$\eta = \frac{\beta Y X}{1 + (2 + Y)X + (1 + Y)(1 + \beta^2)X^2}. \tag{6}$$

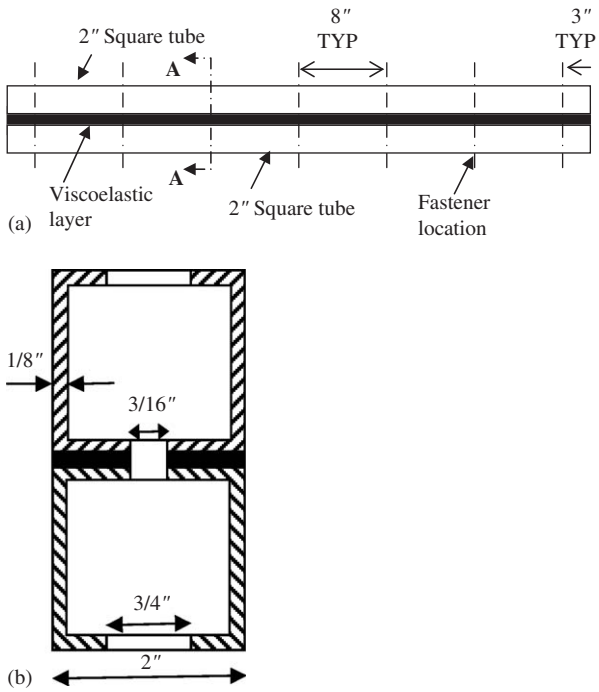

Fig. 3. (a) Layout of beam and fastener locations with (b) cross section of one typical section at stiffener location A–A (enlarged). Stiffeners not shown.

Note that the system loss factor is a function of only three parameters: the viscoelastic material loss factor β, the shear parameter X and the geometric parameter Y. The material loss factor β can be found for a particular frequency using a nomogram or using direct measurements. The geometric parameter, as the name suggests, depends on the geometry and the physical properties of the three layers. The parameter is given by

$$\frac{1}{Y} = \frac{E_1 I_1 + E_3 I_3}{H_{13}^2} \left(\frac{1}{E_1 A_1} + \frac{1}{E_3 A_3} \right), \tag{7}$$

where H_{13} denotes the distance between the neutral axis of the base layer and the constraining layer, and I_i and A_i are the moment of inertia and the cross sectional area of the ith layer, respectively. Furthermore, the shear parameter X is given by

$$X = \frac{G_2 b}{k^2 H_2} \left(\frac{1}{E_1 A_1} + \frac{1}{E_3 A_3} \right). \tag{8}$$

Here, $E_i A_i$ and $E_i I_i$ represent the extensional stiffness and the flexural rigidity, respectively, of the ith layer. G_2 represents the storage modulus (real part of the shear modulus) of the viscoelastic layer. The width and thickness are b and H_2, respectively, of the viscoelastic layer; and k is the

wavenumber of the particular flexural vibration being considered, given by

$$\frac{1}{k^2} = \left(\frac{\lambda}{2\pi}\right)^2 = \frac{1}{\omega}\sqrt{\frac{B}{\mu}}, \tag{9}$$

where λ is the wavelength. The B term denotes the flexural rigidity and μ is the mass per unit length of the structure. Note that the wavenumber depends on the flexural rigidity, which depends on the shear parameter. The shear parameter, of course, also depends on the wavenumber.

In order to estimate the loss factor in the structure design process, an iteration process [9] coded in MATLAB® that quickly yields an accurate prediction of η was used for a particular beam wall thickness. Fig. 4 shows a plot of the loss factor over a range of frequencies for two particular cases. Again, the structure in this analysis is assumed to have no intermediate stiffeners. The first case is for a sandwich structure containing square tubes with wall thicknesses of 1/8″ (3.2 mm). For the other case, the tube sizes are the same with the exception of 1/16″ (1.6 mm) thick walls. A viscoelastic layer of 0.06″ (1.5 mm) thickness is considered for both of these cases.

The first resonance values for the two different wall thicknesses were calculated. The main criterion for selection was to favor the combination that has the first resonance nearest to the frequency where the viscoelastic material, ISODAMP C-1002, as installed in the structure has a large loss factor. The case with 2″ × 2″ cross section, 4.5 foot length and 1/8″ wall thickness was found to be the best choice. This is the configuration described previously in Fig. 3. Fig. 5 shows an end view of the assembled sandwich beam used in the experiments. As mentioned earlier, the iterative complex wavenumber estimation method will be used to measure the system loss factor of the sandwich beam. A brief overview of the experimental set-up is provided next.

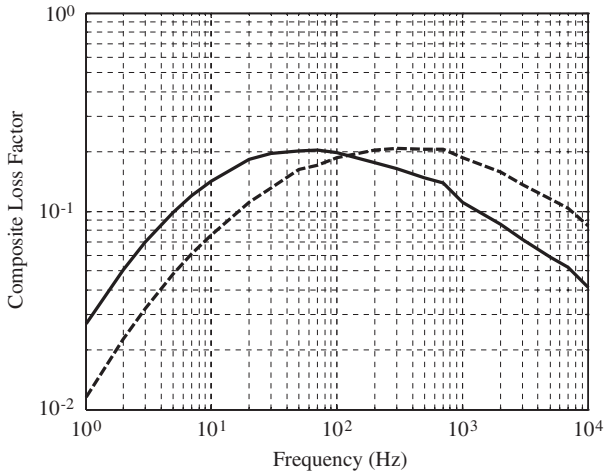

Fig. 4. Composite loss factor for two different beam wall thicknesses; - - - 1/16″, —— 1/8″.

4. Experimental setup

The use of a scanning laser vibrometer system provides relative ease in acquiring a large number of non-contact vibrational measurements over the span of the beam. The experimental set-up incorporating such a system is shown in Fig. 6. Note that the sandwich beam is configured so that the laser beam is normal to the center of the testing surface. This is done to obtain better

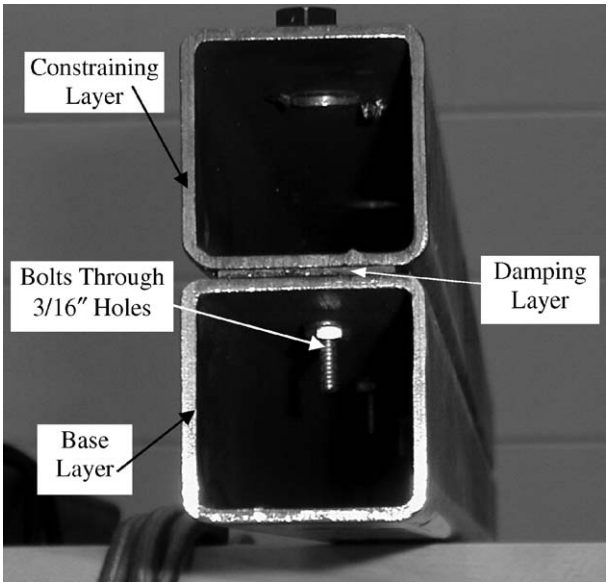

Fig. 5. The composite sandwich beam with bolts after assembly.

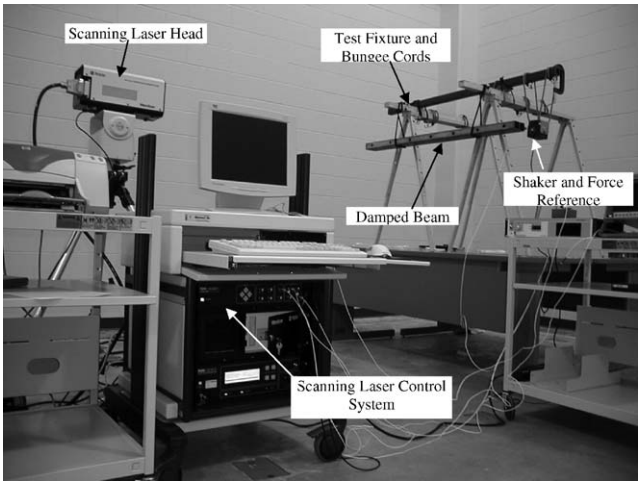

Fig. 6. Experimental setup with the scanning laser system.

reflectivity and hence better signal-to-noise ratio (SNR). It has also been observed that the quality of reflected beam, and hence the SNR, improves substantially when reflective paint is applied on the beam surface. The beam was excited by a random excitation using an electromagnetic shaker. An impedance head is used to measure both input force as well as the velocity at the input. The stinger connecting the shaker to the impedance head is a thin, flexible rod that helps ensure that only uniaxial force is applied to the test specimen. The bolts used to connect the two layers in the specimen (refer to Fig. 5) were fastened with a torque of 30 lb-in (3.4 N m) using a torque wrench. The maximum number of scan-points, which is the same as the number of measurement positions, was 400. The response magnitude and phase were measured at each of these locations using the force sensor as the reference. With this large data set, different measurement points, or subsets, could be selected for the study. Special care was taken to ensure that data were not taken for locations over the holes or on the bungee cords, which were used to support the beam in a free–free like condition. Along with the complex response at each location, the coherence at each point was also stored.

As noted earlier, it will be assumed that the viscoelastically damped beam can be described by a fourth-order differential equation. Some works have shown that a sixth-order equation is sometimes required [10]. Under such conditions, the value for N must be increased to 3. For the assumption of $N = 2$ to hold, the viscoelastic core has to be very stiff in shear. Since this beam has intermediate stiffeners, the core is assumed to be sufficiently stiff. Fig. 7 shows a sample of how well the reconstructed response given by Eq. (2), with k_n determined by the algorithm, matches the measured response for the beam at 1600 Hz. Note that this frequency is the highest frequency considered and is used as the starting point for the analysis. The circles show the measured values of the real and imaginary parts of the response and the line shows the corresponding computed

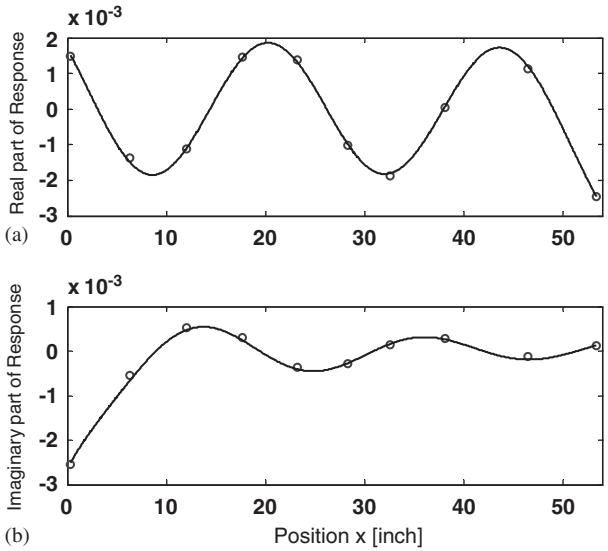

Fig. 7. Comparison of real (a) and imaginary parts (b) of reconstructed response W_m (solid) at 1600 Hz to measured response D_m (circles). Final NMSE for this iteration = 0.18%.

values. This particular case is for 10 equally spaced measurement positions along the length of the beam. The normalized mean square error for this particular iteration is 0.18%. Because the data reconstructed using the wavenumber fitting method matches the experimental results so well for the highest frequency case, the assumption that $N = 2$ seems valid. In other words, the frequencies of interest here appear to be low enough that the assumption of a fourth-order description will be valid. Furthermore, because the goal of the study focuses primarily on relative differences in the predicted value, the validity of this assumption may not be so critical. Further study may be needed with regard to the response of the beam near the boundaries by using a finer grid than shown in the figure. To further investigate such details with regard to the validity of using $N = 2$ for other frequencies and other cases, additional research is needed.

With the assumption that a fourth-order system adequately describes the beam response, the complex wavenumber method can now be used to estimate the loss factor over a range of frequencies. The ability of the method to estimate that loss factor for different measurement sets is discussed in the next section.

5. Results and discussion

The measurement of the response consisted of acquiring the response at 400 points over the length of the beam and over the frequency range of interest. Fig. 8 shows the magnitude of the measured response over the frequency range of interest for each of those 400 measurement locations on the beam. This plot shows that the response is continuous over the length of the measurement aperture. Note that the resonance regions and mode shapes (first three) are clearly indicated in this plot by the light horizontal lines. These first three resonances occur at approximately 250, 600 and 1100 Hz. Fig. 9 shows a real valued wavenumber spectrum found using the response data at each frequency. This plot demonstrates the existence and dispersive nature of flexural waves in the beam. Moreover, resonance frequencies are evidenced by the small

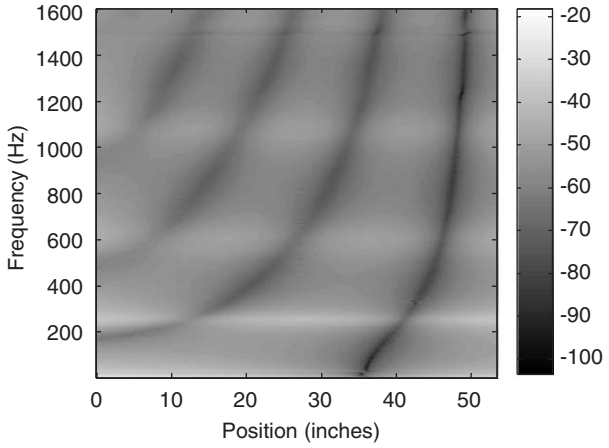

Fig. 8. Response at 400 measurement points along the length of the beam for a range of frequencies. The velocity response is interpolated and plotted in terms of dB. The dB value for a response r is calculated as $20\log_{10}(r)$.

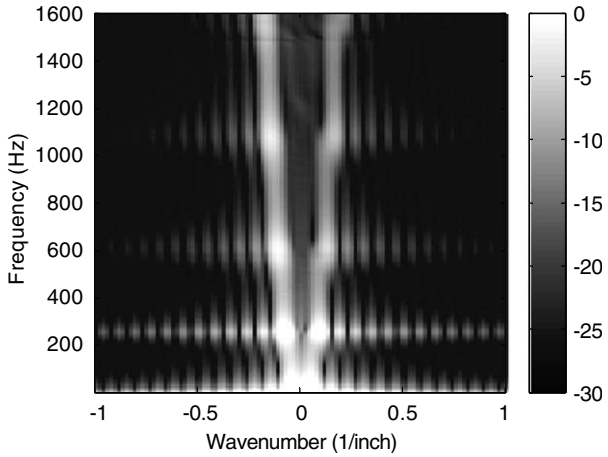

Fig. 9. Variation of wave amplitude with frequency and wavenumber. The velocity response is interpolated and plotted in terms of dB. The dB value for a response r is calculated as $20\log_{10}(r)$.

circular regions of high amplitude. Even though the wavenumbers shown in the plot are purely real valued, the presence of damping behavior is clear from this plot. The negative wavenumbers, which are propagating away from the excitation, have higher amplitudes than those of wave propagating back to the excitation, represented by the positive wavenumbers. Since the reflected wave amplitude from the opposite end is less than the incident wave amplitude, the behavior caused by damping is as expected. For a structure with little or no damping, the amplitude of the waves would be similar for both directions of propagation. Although not very useful in determining the loss factor for the sandwich beam, this data is very useful in verifying the validity of the measurement data set.

The next step was to use the complex response at all 400 points in the wavenumber fitting method to calculate the loss factor. Fig. 10 shows the loss factor and NMSE when using all the 400 points. Note that Fig. 10(b) also shows the loss-factor values for the first three modes obtained using the half-power method. The loss factor was found to be fairly constant over the range of frequencies considered. This may be a characteristic of the particular system under consideration. This may also be due the presence of intermediate stiffeners along the length of the beam specimen. Further studies of the effect of these stiffeners may give additional insight into the constant damping phenomenon. The loss factor curve becomes smoother at frequencies where the NMSE has a lower value. The fluctuations at lower frequencies, such as below the first resonance, may be due to an insufficient measurement aperture to accurately curve fit the longer wavelength. This error may also be caused by an insufficient signal-to-noise ratio at these lower frequencies. Note that the loss factor is obtained for all of the discrete frequencies in this range. The values in this figure are comparable, at least on an order of magnitude, with the values shown in Fig. 4, which were estimated using the basic CLD analysis described above.

To examine the effect of the number of data points, smaller sets of evenly spaced measurements were used while keeping the overall length of the measurement aperture the same. For example, for the 200 measurement-point case, every alternate data point was selected from the 400-point

data set. In using this approach, the length of aperture remains the same but the number of scan points is reduced (the length of the measurement aperture L is kept the same in Eqs. (2) and (4)). The minimum number of measurement points used was five. The results obtained with this exercise indicated that the smoothness of the loss factor curves improved at lower frequencies with increasing number of data points used. When fitting data representing a longer wavelength (lower frequency), small errors in the fit can result in significant differences in the estimated wavenumber. This improvement with an increase in the number of points is due to the fact that the longer wavelength effect is suppressed by using a larger number of data points. Hence, the increased number of data points tends to help reduce curve fitting errors for the wavenumber. As the number of measurement points used increases, the measurement time also increases, which will become clearer in later discussions. As a result, one would like to find a compromise between the degree of accuracy required and the acquisition time needed.

Since it is apparent that the results can depend on the number of measurements used, the loss factor value for a few particular frequencies was examined. Considering the 400-point case as the reference, Table 1 shows the loss factor at each of the first three resonance frequencies. The

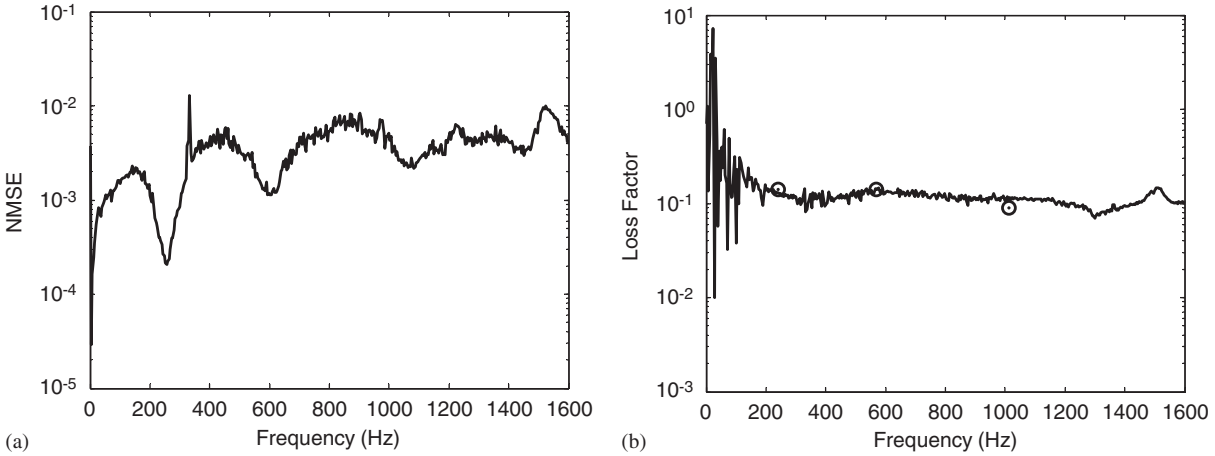

Fig. 10. NMSE and loss factor for 400 points. Circles in (b) show half-power values for first three modes.

Table 1
Loss factor with different number of measurement positions

Mode	Number of points													
	5		10		20		50		100		200		400	
	η	Δ%	η	Δ%	η	Δ%	η	Δ%	η	Δ%	η	Δ%	η	Δ%
1	0.07	18.25	0.08	9.47	0.09	6.57	0.09	6.02	0.09	2.81	0.08	7.91	0.09	—
2	0.02	82.14	0.14	31.06	0.14	28.09	0.14	25.14	0.07	33.69	0.11	2.70	0.11	—
3	0.13	36.40	0.10	2.54	0.10	4.98	0.10	6.59	0.10	5.25	0.10	7.62	0.10	—

percent difference shown in this table ($\Delta\%$) is relative to the 400-point measurement, with the assumption that the value for 400 points is the correct value. Note that in general the loss factor converges to a constant value as the number of points used in the analysis increases. Furthermore, the results for the first and third resonance frequencies tend to be more consistent.

Since the number of points affects the accuracy of this method, a more comprehensive study can be conducted at the first three resonant frequencies. The percent difference in loss factor versus the number of data points for these three frequencies is shown in Fig. 11. The figure also shows the average coherence, which was calculated by taking the average over all the measurement locations for each frequency. Again, the 400-point case is considered as a reference upon which the percent difference value is calculated. Note that there are some fluctuations in the curve as the number of points increases, especially for the second resonance. Generally speaking, when the average coherence for all the data points decreases, as shown in Fig. 11(b), the loss factor error increases. Also note that for fewer points (<100), whenever the coherence value decreases, the percent difference in loss factor increases. As a result, very good results can be obtained with just a few good measurement points (≈ 10) provided the average coherence for those points is sufficiently high. Fig. 11(a) also shows the acquisition time required based on the number of data points used. This acquisition time includes only the time required by the vibrometer system to take the measurements. While considering time as a factor, one should also take into account the post-processing time. That time includes the time required to transfer the measurement data of all the scan points as well as the time for the PC and MATLAB® to calculate the loss factor at each frequency. These times would depend more on the particular computer used. For the Gateway computer (500 MHz, 392 MB RAM) used in this study, the time for loss factor calculation at all the frequencies varied from 30 s for 10 points to 5 min for 400 points. Note that even though there is a substantial time difference (10 times), the time for 400 points is not very significant. Nevertheless, it was found that the initial wavenumber estimation takes a considerable amount of time. For the somewhat crude approach used here, this time varied from approximately 8 min for 10 points to 12 h for 400 points. Once the initial guess for the 400 points case is calculated, no other guess values are needed as the next frequency uses the result at the previous frequency as the guess.

It appears that the loss factor errors may be due to the coherence of the measured data. The loss factor values are very sensitive to coherence when the number of measurements points is smaller. To verify this inference, the loss factors for three different combinations of 60-data points sets were analyzed. The first case was for 60 arbitrarily chosen points. The second and third cases were

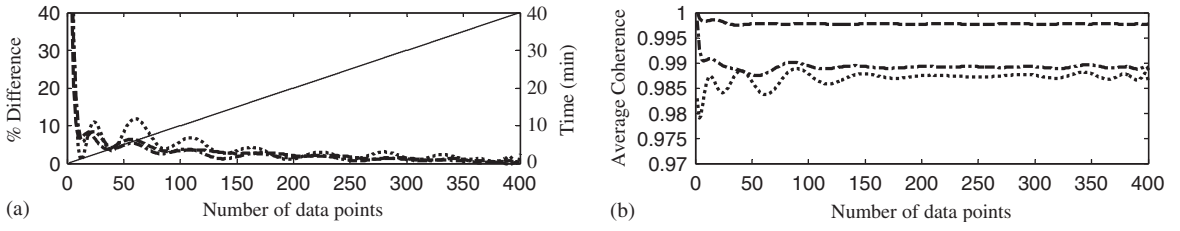

Fig. 11. Changes in loss factor (a) and coherence (b) with number of data points; --- Mode 1, · · · · Mode 2, - · - · - · - Mode 3, —— acquisition time (min).

for the 60 poorest and best coherence valued data points, respectively. The length of aperture L is still the same. It was found that the loss factor curve for the 60 best coherence points was significantly smoother as compared to the other two cases. Generally speaking, there is a benefit to having fewer points, especially if the average coherence is higher. This finding agrees with the conclusions made above.

In the discussion above for Fig. 11, it was assumed that the 400 point case provided the best result and could therefore be used as a reference for the comparison. A better reference would be a case in which all of the points have a relatively high coherence, such as the 60 best-points case considered above. It should be reiterated that these 60 points were almost evenly spaced but selected based purely on coherence levels. By using the loss factors for the 60 "best" data points as a reference, the difference in the loss factor values for different numbers of evenly spaced data points was recalculated. Although not shown here, it was observed that the percentage difference does not necessarily decrease by incorporating more evenly spaced data. This confirms the fact that using fewer points with higher coherence can be better than using more points with poorer coherence. Hence, adding more points does not necessarily counteract a low coherence and guarantee better results. For the first mode, for example, 10 points spanning the aperture with high coherence was found to be better than 400 points with poor SNR. As the vibration shape of the beam becomes more complex, such as for the higher modes, more data points may be needed due to the fact that more points are needed to accurately capture the shape of the structure.

It is also noted from the experimental results that there seems to be no effect on the loss factor that can specifically be attributed to the intermediate fasteners. This may be because the stiffness of bolts used may be small as compared to that of the composite beam. Investigation into the effect of the number of bolts and the magnitude of torquing may give further insight in future research.

6. Summary

A relatively new damping measurement technique is evaluated in this work. This new technique estimates the complex wavenumber for a particular frequency by matching the experimental vibratory response to the analytical response. A viscoelastically damped sandwich beam with its layers coupled with adhesive as well as fasteners along its length is used for the experiments. It should be noted that even though a beam bolted with fasteners is used for the present study, this damping measurement technique might be used as effectively for any beam configuration. By using subsets from the large data set, the impact of the number of points as well as the coherence of those data points on the accuracy of the wavenumber method could be examined. The complex wavenumber iterative method was found to be more sensitive to coherence of the measured data points than the number of measurement points. However, at higher frequencies, the effect of the higher number of scan points overwhelms the effect of coherence. Therefore, one should use a greater number of data points at higher frequencies if the SNR in the measured data is low. It should be noted that the number of measurement locations needs to be considered only while using this iterative algorithm. Moreover, when using this method, it is easier to use the vibrometer system than conventional accelerometers due to the ease provided by this system in acquiring data at a large number of locations. For the case considered here, an accuracy of 10% can be attained

with the use of at least 10 data points with good coherence. These data points should have very high coherence values (>0.995) and should span the length of the beam. One should use more points when an accuracy of better than 10% relative to the reference case is desired, or at higher frequencies.

References

[1] J.G. McDaniel, W.S. Shepard Jr., Estimation of structural wave parameters from spatially sparse response measurements, *Journal of Acoustical Society of America* 108 (2000) 1674–1682.
[2] M.J. Yan, E.H. Dowell, High damping measurements and a preliminary evaluation of an equation for constrained-layer damping, *AIAA Journal* 11 (1973) 388–390.
[3] E.M. Kerwin, Damping of flexural waves by a constrained viscoelastic layer, *Journal of Acoustical Society of America* 31 (1959) 952–962.
[4] E.M. Kerwin, R.J. Mcquillan, *Plate damping by a constrained viscoelastic layer: Partial coverage and boundary effects*, Bolt Beranek and Newman Inc., 1960 No. 760.
[5] D.J. Mead, The vibration characteristics of damped sandwich plates with stiffeners and various boundary conditions, *Strojnicky Casopis* 22 (1971) 53–67.
[6] S. Markus, V. Oravsky, O. Simkova, Damping properties of sandwich beams with local shearing prevention, *Acustica* 31 (1974) 138.
[7] L. Cremer, M. Heckl, The complex modulus of elasticity, in: *Structure-Borne Sound: Structural Vibrations and Sound Radiation at Audio Frequencies*, Springer, Berlin, NY, 1988, pp. 199–204.
[8] A.E.S. Composites Damping Materials (www.earsc.com).
[9] E.E. Ungar, Loss factors of viscoelastically damped beam structures, *Journal of Acoustical Society of America* 34 (1962) 1082–1089.
[10] D.J. Mead, A comparison of some equations for the flexural vibration of damped sandwich beams, *Journal of Sound and Vibration* 83 (1982) 363–377.